

Quantum localized modes in capacitively coupled Josephson-junction qubits

R. A. Pinto and S. Flach

Max-Planck-Institut für Physik komplexer Systeme, Nöthnitzer Str. 38, 01187 Dresden, Germany

(Dated: May 26, 2019)

We consider the quantum dynamics of excitations in a system of two capacitively coupled Josephson-junction qubits. Quantum breather states are found in the middle of the energy spectrum of the confined nonescaping states of the system. They are characterized by a strong excitation of one junction. These states perform slow tunneling motion from one junction to the other, while keeping their coherent nature. The tunneling time sensitively depends on the initial excitation energy. By using an external bias as a control parameter, the tunneling time can be varied with respect to the escape time and the experimentally limited coherence time. Thus one can control the flow of quantum excitations between the two junctions.

PACS numbers: 63.20.Pw, 74.50.+r, 85.25.Cp, 63.20.Ry

Josephson junctions are the subject of extensive studies in quantum information experiments because they possess two attractive properties: they are nonlinear devices, and also show macroscopic quantum behavior [1, 2, 3]. The dynamics of a biased Josephson junction (JJ) is analogous to the dynamics of a particle with a mass proportional to the junction capacitance C_J , moving on a tilted washboard potential

$$U(\varphi) = -I_c \frac{\Phi_0}{2\pi} \cos \varphi - I_b \varphi \frac{\Phi_0}{2\pi}, \quad (1)$$

which is sketched in Fig.1-b. Here φ is the phase difference between the macroscopic wave functions in both superconducting electrodes of the junction, I_c is the critical current of the junction, and $\Phi_0 = h/2e$ the flux quantum. When the energy of the particle is large enough to overcome the barrier ΔU (that depends on the bias current I_b) it escapes and moves down the potential, switching the junction into a resistive state with a nonzero voltage proportional to $\dot{\varphi}$. Quantization of the system leads to discrete energy levels inside the wells in the potential, which are nonequidistant because of the anharmonicity. Note that even if there is not enough energy to classically overcome the barrier, the particle may perform a quantum escape and tunnel outside the well, thus switching the junction into the resistive state [1]. Thus each state inside the well is characterized by a bias and a state-dependent inverse lifetime, or escape rate.

Progress on manipulation of quantum JJs includes spectroscopic analysis, better isolation schemes, and simultaneous measurement techniques [2, 3, 4, 5], and paves the way for using them as JJ qubits in arrays for experiments on processing quantum information. Typically the first two or three quantum levels of one junction are used as quantum bits. Since the levels are nonequidistant, they can be separately excited by applying microwave pulses.

So far, the studies on JJ qubits focused on low energy excitations involving the first few energy levels of the junctions. Larger energies in the quantum dynamics of JJs give rise to new phenomena that can be observed by using the already developed techniques for quantum

information experiments. For instance, it was suggested that Josephson junction qubits operated at high energies may be used for experiments on quantum chaos [6, 7, 8].

In this work we consider large energy excitations in a system of two capacitively coupled JJ qubits [9, 10, 11]. We study the time evolution of states when initially only one of the junctions was excited. In the low energy sector such a state will lead to beating with a beating time depending solely on the strength of the capacitive coupling. For larger excitation energies the states perform slow tunneling motion, where the tunneling time sensitively depends on the initial energy, in contrast to the low energy beating time. We calculate the eigenstates and the spectrum of the system, and identify quantum breather states (QB), which are weakly splitted tunneling pairs of states [12, 13, 14, 15, 16]. These eigenstates appear in the middle of the energy spectrum of the system and are characterized by correlations between the two junctions - if one of them is strongly excited, the other one is not, and vice versa. By exciting one of the junctions to a large energy, we strongly overlap with QB tunneling states. Consequently we trap the excitation on the initially excited junction on a time scale which sensitively depends on the amount of energy excited, and on the applied bias.

The system is sketched in Fig.1-a: two JJ qubits are coupled by a capacitance C_c , and they are biased by the same current I_b . The strength of the coupling due to the capacitor is $\zeta = C_c/(C_c + C_J)$. The Hamiltonian of the system is

$$H = \frac{P_1^2}{2m} + \frac{P_2^2}{2m} + U(\varphi_1) + U(\varphi_2) + \frac{\zeta}{m} P_1 P_2, \quad (2)$$

where

$$m = C_J(1 + \zeta) \left(\frac{\Phi_0}{2\pi} \right)^2, \quad (3)$$

$$P_1 = (C_c + C_J) \left(\frac{\Phi_0}{2\pi} \right)^2 (\dot{\varphi}_1 - \zeta \dot{\varphi}_2), \quad (4)$$

$$P_2 = (C_c + C_J) \left(\frac{\Phi_0}{2\pi} \right)^2 (\dot{\varphi}_2 - \zeta \dot{\varphi}_1). \quad (5)$$

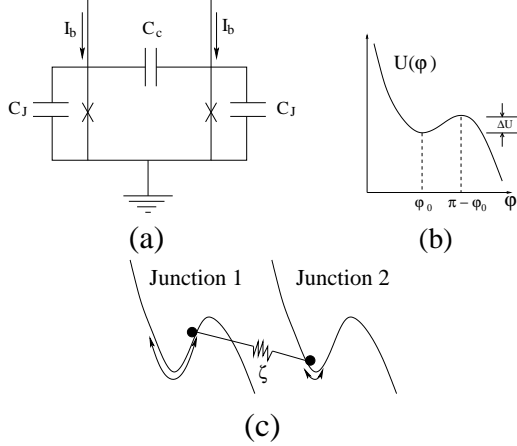


FIG. 1: (a) Circuit diagram for two ideal capacitively coupled JJs. (b) Sketch of the washboard potential for a single current-biased JJ. (c) Sketch of a breather solution in the classical dynamics of the system.

When the junctions are in the superconducting state, they behave like two coupled anharmonic oscillators. The plasma frequency is $\omega_p = \sqrt{2\pi I_c/\Phi_0 C_J(1 + \zeta)[1 - \gamma^2]^{1/4}}$, and $\gamma = I_b/I_c$ is the normalized bias current. The classical equations of motion of the system admit breather solutions [17], which are time periodic, and for which the energy is localized predominantly on one of the junctions (Fig.1-c). These orbits are numerically computed with high accuracy by using Newton algorithms [18, 19].

In the quantum case we compute the energy eigenvalues and the eigenstates of the system. We neglect quantum escape for states which will not escape in the classical limit. Thus we use a simple model for the single JJ qubit, where the potential energy is changed by adding a hard wall which prevents escape:

$$U_q(\varphi) = \begin{cases} U(\varphi) & \text{if } \varphi \leq \pi - \varphi_0 \\ \infty & \text{if } \varphi > \pi - \varphi_0 \end{cases}, \quad (6)$$

where $\varphi_0 = \arcsin \gamma$ is the position of the minimum of the potential and $\pi - \varphi_0$ gives the position of the first maximum to the right from the equilibrium position φ_0 (Fig.1-b). We will later compare the obtained tunneling times with the true state dependent escape times.

The Hamiltonian of the two-junctions system is given by

$$\hat{H} = \hat{H}_1 + \hat{H}_2 + \frac{\zeta}{m} \hat{V}, \quad (7)$$

where $\hat{H}_i = \hat{P}_i^2/2m + U_q(\hat{\varphi}_i)$ is the single-junction Hamiltonian and $\hat{V} = \hat{P}_1 \hat{P}_2$ is the interaction that couples the junctions. The eigenvalues ε_{n_i} and eigenstates $|n_i\rangle$ of the single-junction Hamiltonian \hat{H}_i were computed by using the Fourier grid Hamiltonian method [20]. Note that $|n_i\rangle$ is also an eigenstate of the number operator \hat{n}_i with eigenvalue n_i . In the harmonic approximation $\hat{n}_i = \hat{a}_i^\dagger \hat{a}_i$,

where \hat{a}_i^\dagger and \hat{a}_i are the bosonic creation and annihilation operators. Since only states with energies below the classical escape energy (barrier) are taken into account, the computed spectra have a finite upper bound. The perturbation \hat{V} does not conserve the total number of quanta $n_1 + n_2$, as seen from the dependence of the momentum operators on the bosonic creation and annihilation operators in the harmonic approximation: $\hat{P}_{1,2} = (\Phi_0/2\pi)\sqrt{(1 + \zeta)C_J \hbar \omega_p/2}(\hat{a}_{1,2} - \hat{a}_{1,2}^\dagger)/i$.

The Hamiltonian matrix is written in the basis of product states of the single-junction problem $\{|n_1, n_2\rangle = |n_1\rangle \otimes |n_2\rangle\}$. The invariance of the Hamiltonian under permutation of the junction labels allows us to use symmetric and antisymmetric basis states

$$|n_1, n_2\rangle_{S,A} = \frac{1}{\sqrt{2}}(|n_1, n_2\rangle \pm |n_2, n_1\rangle) \quad (8)$$

to reduce the full Hamiltonian matrix to two smaller symmetric and antisymmetric decompositions of \hat{H} , which after diagonalization respectively give the symmetric and antisymmetric eigenstates of the system.

In order to identify quantum breather states, whose corresponding classical orbits are characterized by energy localization, we define the correlation functions:

$$f_\mu(1, 2) = \langle \hat{n}_1 \hat{n}_2 \rangle_\mu \quad (9)$$

$$f_\mu(1, 1) = \langle \hat{n}_1^2 \rangle_\mu, \quad (10)$$

where $\langle \hat{A} \rangle_\mu = \langle \chi_\mu | \hat{A} | \chi_\mu \rangle$, $\{|\chi_\mu\rangle\}$ being the set of eigenstates of the system. The ratio $0 \leq f_\mu(1, 2)/f_\mu(1, 1) \leq 1$ measures the site correlation of quanta: it is small when quanta are site-correlated (when there are many quanta on one junction there are almost none on the other one) and close to one otherwise.

In Fig.2 we show the nearest neighbor energy spacing (splitting) and the correlation function of the eigenstates. For this, and all the rest, we used $I_c = 13.3 \mu\text{A}$, $C_J = 4.3 \text{ pF}$, and $\zeta = 0.1$, which are typical values in experiments. We see that in the central part of the spectrum the energy splitting becomes small in comparison to the average. The corresponding pairs of eigenstates, which are tunneling pairs, are site correlated, and thus QBs. In these states many quanta are localized on one junction and the tunneling time of such an excitation from one junction to the other (given by the inverse energy splitting between the eigenstates of the pair) can be exponentially large and depends sensitively on the number of quanta excited.

The fact that the most site correlated eigenstates occur in the central part of the energy spectrum may be easily explained as follows: Let N be the highest excited state in a single junction, with a corresponding maximum energy ΔU (Fig.1). For two junctions the energy of the system with both junctions in the N -th state is $2\Delta U$, which roughly is the width of the full spectrum. Thus states of the form $|N, 0\rangle$ and $|0, N\rangle$ that have energy ΔU are located roughly in the middle.

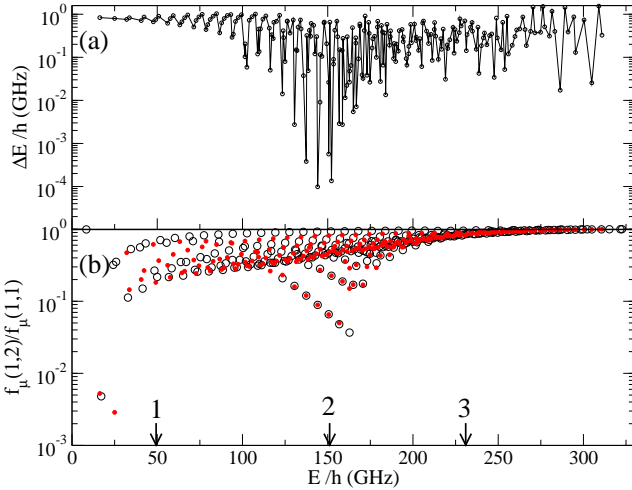


FIG. 2: (Color online) (a) Energy splitting and (b) correlation function vs. energy for the two-junctions system (open circles, symmetric eigenstates; filled circles, antisymmetric eigenstates). The labeled arrows mark the energy corresponding to the peak of the spectral intensity in Fig.3-b, d, and f (see text). The parameters are $\gamma = 0.945$ and $\zeta = 0.1$ (22 levels per junction).

With the eigenvalues and eigenstates we compute the time evolution of different initially localized excitations, and the expectation value of the number of quanta at each junction $\langle \hat{n}_i \rangle(t) = \langle \Psi(t) | \hat{n}_i | \Psi(t) \rangle$. Results are shown in Fig.3a, c, and e. Also we compute the spectral intensity $I_\mu^0 = |\langle \chi_\mu | \Psi_0 \rangle|^2$, which measures how strong the initial state $|\Psi_0\rangle$ overlaps with the eigenstates. Results are shown in Fig.3-b, d, and f, where we can see a peak in each case, which corresponds to the arrows in Fig.2-b. We can see that the initial state $|\Psi_0\rangle = |0, 5\rangle$ overlaps with site correlated eigenstates with an energy splitting between them being relatively large and hence the tunneling time of the initially localized excitation is short. For the case $|\Psi_0\rangle = |0, 19\rangle$ QBs are excited: The excitation overlaps strongly with tunneling pairs of eigenstates in the central part of the spectrum, which are site correlated and nearly degenerate. The tunneling time of such an excitation is very long, and thus keeps the quanta localized on their initial excitation site for corresponding times. Finally the initial state $|\Psi_0\rangle = |9, 19\rangle$ overlaps with weakly site correlated eigenstates with large energy splitting. Hence the tunneling time is short.

We tested whether a (coherent or incoherent) spreading of the initial state over a suitable energy window affects the results discussed above. For instance instead of using the basis state $|0, 19\rangle$ as the initial state (Fig.3-c,d), we superposed the basis states $|0, 20\rangle$, $|0, 19\rangle$, $|0, 18\rangle$, and $|0, 17\rangle$. We found that the results qualitatively do not change.

The experimental observation of QBs may be possible by using the scheme used by McDermondt *et al* for simultaneous state measurement of coupled Josephson phase qubits[4], where by applying microwave pulses

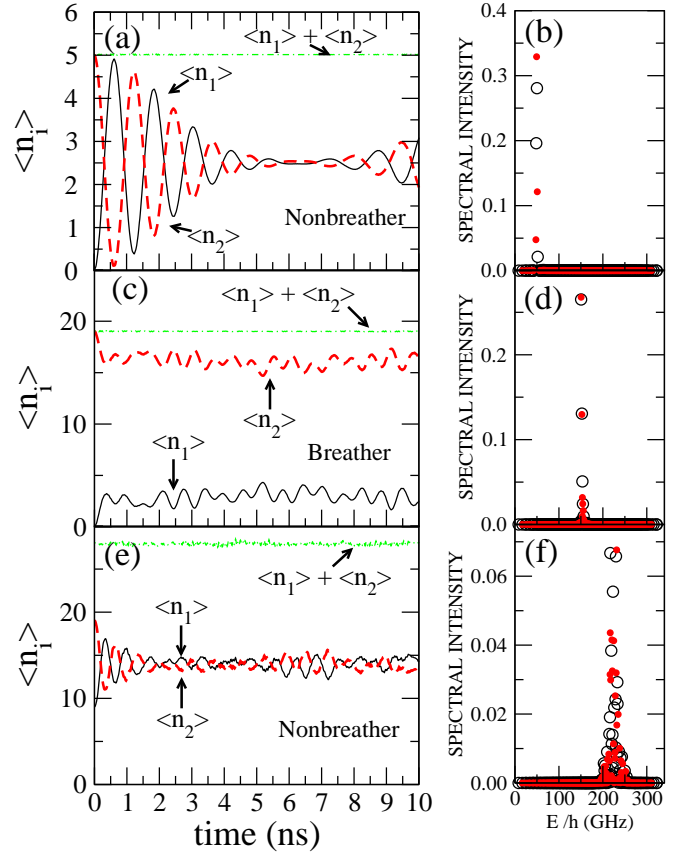


FIG. 3: (Color online) Time evolution of expectation values of the number of quanta at each junction for different initial excitations and their corresponding spectral intensity. (a) and (b): $|\Psi_0\rangle = |0, 5\rangle$; (c) and (d): $|\Psi_0\rangle = |0, 19\rangle$; (e) and (f): $|\Psi_0\rangle = |9, 19\rangle$. Open circles, symmetric eigenstates; filled circles, antisymmetric eigenstates. The energies of the peaks in the spectral intensity are marked by labeled arrows in Fig.2-b (see text). The parameters are $\gamma = 0.945$ and $\zeta = 0.1$ (22 levels per junction).

the time evolution of the occupation probabilities in the qubits is measured. By applying a first microwave pulse on one of the junctions we excite it into a high energy single-junction state with energy ε_l and leave the other one in the ground state. In this way we have an initial state similar to that shown in Fig.3-c and d. After a variable period of time we apply simultaneous microwave pulses to the junctions. The frequency of this pulse is slightly higher than $(\Delta U - \varepsilon_l)/\hbar$, which is the frequency necessary to overcome the energy barrier ΔU from the single-junction level ε_l . Then we test which junction switches to the resistive state. By repeating the measuring many times we obtain the populations in the junctions as a function of the time between the initial pulse and the simultaneous measuring pulses.

Let us discuss the so far neglected quantum escape. For that we computed τ_{escape} by using the semiclassical

TABLE I: Escape times for metastable states in a single JJ τ_{escape} estimated by formula (11), and tunneling time of the initial excitation $|\Psi(0)\rangle = |0, l\rangle$ between the two junctions τ_{tunnel} estimated from energy splittings.

l	τ_{tunnel} (ns)	τ_{escape} (ns)
20	348	42
19	1.8×10^3	3.5×10^3
18	10.16×10^3	503.2×10^3
17	2.3×10^3	71.2×10^6
16	366	1.62×10^9

formula [21]

$$\tau_{\text{escape}}^{-1}(\varepsilon) = \frac{\omega(\varepsilon)}{2\pi} \exp \left\{ -\frac{2}{\hbar} \int_a^b p(\varphi) d\varphi \right\}, \quad (11)$$

where a and b are the turning points of the classical motion in the reversed potential at $U(\varphi) = \varepsilon$, $p(\varphi) = \sqrt{2[U(\varphi) - \varepsilon]}$, and $\omega(\varepsilon)/2\pi$ is the frequency of the oscillations inside the initial well. In table I we show the escape time from different metastable states, and we compare it with the tunneling time τ_{tunnel} of an initial excitation $|\Psi(0)\rangle = |0, l\rangle$ between the two junctions, estimated from the energy splitting of the (symmetric-antisymmetric) pair of eigenstates with the largest overlap with the initial excitation. We see that for $l = 19$, where we excite QBs, the escape time is long enough for observing at least one tunneling exchange between the two junctions before escaping to the resistive state. Note that the cases $l = 18$ and 17 also excite QBs which would show even more tunneling exchanges before escaping. So we expect that escaping to the resistive state will not prevent from the experimental observation of QDB excitations.

Another phenomenon that was not taken into account in our quantum model is decoherence. To be able to observe tunneling between the junctions the coherence

time has to be longer than the shortest tunneling time between the junctions, which is of the order of 1 ns in the cases shown in Fig.3-a and e. In the experiment shown in [9] using a few levels per junction a coherence time of the same order was obtained. However, we expect that improvements in experiments [2] will lead to longer coherence times.

In summary, we have studied the classical and quantum dynamics of high-energy localized excitations in a system of two capacitively coupled JJ qubits. In the classical case the equations of motion admit time periodic localized excitations (discrete breathers) which can be numerically computed. For the quantum case we showed that excitation of one of the junctions to a high level leaving the another junction in the ground state lead to a QB with long lifetime. This is possible because the excitation overlaps strongly with tunneling-pair eigenstates which live in the central part of the energy spectrum and localize energy on one of the junctions. This result would not qualitatively change if we excite a (coherent or incoherent) superposition of several product basis states instead of only one. We showed that with the available techniques for manipulating JJ qubits the experimental observation of QDB excitations is possible. Escaping to the resistive state of the junctions (which together with decoherence was not taken into account in our quantum model) would not prevent us from doing that, and we expect that improvements on isolation techniques of qubits will lead to long enough coherence times, such that the phenomena we described in this work will be clearly observed. That would ultimately pave the way of a controlled stirring of quanta on networks of JJs.

Acknowledgments

This work was supported by the DFG (grant No. FL200/8) and by the ESF network-programme AQDJJ.

[1] Likharev, K. K. *Dynamics of Josephson junctions and circuits* (Gordon and Breach Science Publishers, Philadelphia, 1984).

[2] *Quantum Computing and Quantum Bits in Mesoscopic Systems*, edited by A. Leggett *et al* (Kluwer Academic/Plenum Publishers, New York, 2004).

[3] *Les Houches 2003, Quantum Entanglement and Information Processing*, edited by D. Estève *et al* (Elsevier, Amsterdam, 2004).

[4] R. McDermott *et al*, *Science* **307**, 1299 (2005).

[5] J. M. Martinis *et al*, *Phys. Rev. Lett.* **55**, 1543 (1985).

[6] R. Graham *et al*, *Phys. Rev. Lett.* **67**, 255 (1991).

[7] S. Montangero *et al*, *Europhys. Lett.* **71**, 893 (2005).

[8] E. N. Pozzo *et al*, *cond-mat/0601698*.

[9] A. J. Berkley *et al*, *Science* **300**, 1548 (2003).

[10] P. R. Johnson *et al*, *Phys. Rev. B* **67**, 020509(R) (2003).

[11] A. Blais *et al*, *Phys. Rev. Lett.* **90**, 127901 (2003).

[12] A. C. Scott *et al*, *Phisica* **78D**, 194 (1994).

[13] V. Fleurov, *Chaos* **13**, 676 (2003).

[14] W. Z. Wang *et al*, *Phys. Rev. Lett.* **76**, 3598 (1996).

[15] S. Flach *et al*, *J. Phys.: Cond. Matt.* **9**, 7039 (1997).

[16] R. A. Pinto *et al*, *Phys. Rev. A* **73**, 022717 (2006).

[17] S. Flach *et al*, *Phys. Rep.* **295**, 181 (1998).

[18] *Energy Localization and Transfer*, Edited by T. Dauxois *et al*, (World Scientific, 2004).

[19] D. Chen *et al*, *Phys. Rev. Lett.* **77**, 4776 (1996).

[20] C. Clay Marston *et al*, *J. Chem. Phys.* **91**, 3571 (1989).

[21] Landau, L. D. and Lifshitz, E. M. *Quantum Mechanics* (Pergamon London, 1958).